Direct determination of atomic structure of large-indexed carbon nanotubes by electron diffraction: application to double-walled nanotubes

IOP PUBLISHING JOURNAL OF PHYSICS D: APPLIED PHYSICS

J. Phys. D: Appl. Phys. **42** (2009) 125412 (6pp) doi:10.1088/0022-3727/42/12/125412

Direct determination of atomic structure of large-indexed carbon nanotubes by electron diffraction: application to double-walled nanotubes

Kaihui Liu, Zhi Xu, Wenlong Wang, Peng Gao, Wangyang Fu, Xuedong Bai[1] and Enge Wang[1]

Beijing National Laboratory for Condensed Matter Physics, Institute of Physics, Chinese Academy of Sciences, Box 603, Beijing 100190, People's Republic of China

E-mail: xdbai@aphy.iphy.ac.cn and egwang@aphy.iphy.ac.cn

Received 23 December 2008, in final form 29 December 2008
Published 5 June 2009
Online at stacks.iop.org/JPhysD/42/125412

Abstract

We report a method for the determination of the chiral indices of large-indexed carbon nanotubes by electron diffraction. By the use of this method, the index assignment errors, originating from the tilt of a nanotube with respect to the incident electron beam, can be directly specified. As an example, the chiral indices of a double-walled nanotubes with index up to 80 and under a high tilt angle of as large as 20° have been accurately identified. Only the data of the maximum peaks of the diffraction layer lines are required in the study, which makes the chiral index determination much easier based on the common diffraction patterns.

1. Introduction

With the unique structure and fascinating properties, carbon nanotubes (CNTs) have attracted a great deal of interest both in fundamental science and in practical technology [1, 2]. Since the physical properties of CNTs are extremely sensitive to their atomic structure—uniquely indexed with the chiral indices (n, m) that describe the CNT construction as a rolled-up graphene sheet [3, 4], a critical issue in CNT study is the accurate (n, m) identification of every shell for a given individual nanotube [5–7]. During the past few years, due to the continued experimental and theoretical efforts, electron diffraction (ED) has been emerging as a powerful technique for determining the (n, m) indices of single-walled nanotubes (SWNTs) with usually relatively small indices of less than 30 [8–22]. However, as for the large-indexed CNTs, such as the double-walled nanotubes (DWNTs), the accurate (n, m) assignment is still a big challenge [23–27].

Basically, the current state of the art in determining the chiral indices of nanotubes from their electron diffraction patterns (EDPs) can be categorized into two classes: one is based on the tube diameter and the chiral angle [15–17, 24–27], and the other is based on the Bessel function fitting of the distribution of diffraction layer-line intensities [18–21]. As for the former method, the diameter D and the chiral angle α of each tube shell are first determined. Then among the possible combinations, the (n, m) indices, which are exclusively in line with (D, α), can be identified. In this method, both D and α must be determined with high accuracy, and only a slight error in either D or α may lead to an ambiguity in indexing (n, m) [15–17]. In practice, there might be several (n, m) combinations that will match (D, α) within the errors of D and α. For nanotubes with large indices, e.g. more than 30, their error range of (D, α) is much larger than that of small-indexed nanotubes [26]. Thus, it becomes difficult for this method to accurately determine the (n, m) indices of large-indexed nanotubes. As for the latter method, the chiral indices are retrieved from the orders of Bessel functions that fit the intensity distribution of certain diffraction layer lines. However, theoretically, this fitting is valid only for normal electron incidence with respect to nanotubes [18–21]. In practice with tube inclination, the Bessel function fitting will result in the inaccurate determination of the chiral index. And the errors of chiral indices will become much larger with increasing nanotube indices, because the corresponding

[1] Authors to whom any correspondence should be addressed.

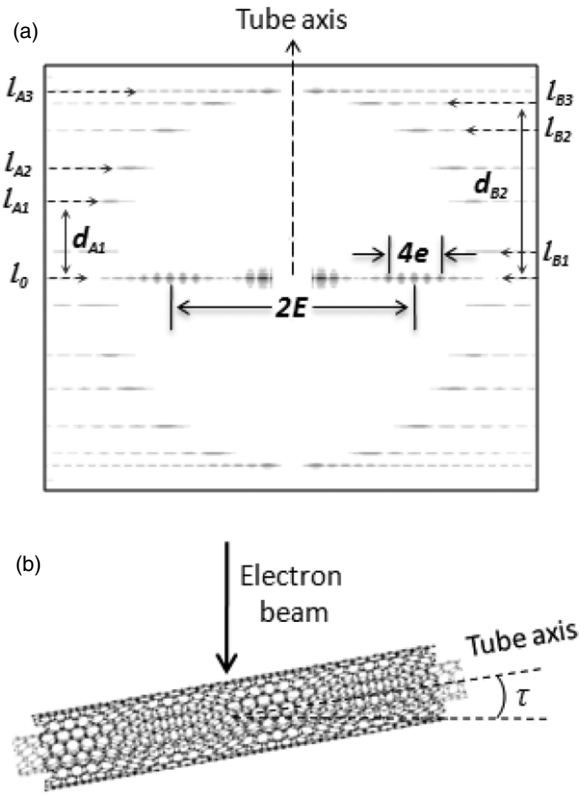

Figure 1. (*a*) Simulated EDP from a (40, 5)/(25, 15) DWNT in the case of normal electron beam incidence. Two groups of layer lines $[l_0, l_{A1}, l_{A2}, l_{A3}]$ and $[l_0, l_{B1}, l_{B2}, l_{B3}]$, layer-line spacing d_{A1} and d_{B2}, and the oscillation periods of e and E in layer-line l_0 are schematically illustrated. (*b*) Schematic expression of the tilt angle τ of the nanotube with respect to the incident electron beam.

high-order Bessel functions differ very slightly among each other [18]. Typically, this method is effective in determining the (n, m) indices of nanotubes with an index less than 30 under a small tilt angle ($<6^\circ$) [19]. In addition, several peak positions and intensities in the diffraction layer lines should be of high precision in this method, which makes it incapable for the EDPs with low pixel resolution [20].

In this paper, we develop a new approach for the accurate chiral identification of large-indexed DWNTs from their EDPs. And our method is also applicable for SWNTs and other few-walled nanotubes. The tilt-effect errors in (n, m) assignment are precisely specified, and the tilt angle is also evaluated simultaneously. The accuracy in determining (n, m) indices of large-indexed DWNTs under a high tilt angle is validated from both the simulated and the experimental diffraction patterns.

2. Method

Figure 1(*a*) shows a simulated EDP from a (40, 5)/(25, 15) DWNT in the case of normal electron beam incidence. Here, we designate the chiral indices of a DWNT as $(n_o, m_o)/(n_i, m_i)$, where subscripts 'o' and 'i' stand for outer and inner shells, respectively. It is seen that the diffraction pattern comprises several layer lines; and these layer lines can be divided into two groups as $[l_0, l_{A1}, l_{A2}, l_{A3}]$ (group A) and $[l_0, l_{B1}, l_{B2}, l_{B3}]$ (group B), originating from the two-shell structure [23]. The intensity and location features of these layer lines are unique for a given DWNT and will be used to determine its (n, m) indices.

First, the outer (D_o) and inner diameters (D_i) will be extracted from the intensity profile of layer-line l_0. Based on the concentric structure of DWNTs, the intensity distribution in layer-line l_0 oscillates with a small period $e = 1/\bar{D}$, within an oscillatory envelope of a large period $E = 1/\delta D$ [25], where $\bar{D}$ is the mean diameter $[(D_o + D_i)/2]$, and δD is the intershell distance $[(D_o - D_i)/2]$. The outer and inner diameters can be deduced from the two periods by an expression:

$$D_o = 1/e + 1/E, \qquad D_i = 1/e - 1/E. \tag{1}$$

Secondly, we employ the difference in the diffraction intensities to link the two groups of layer lines with the outer and inner tube shells. This difference comes from the different numbers of atoms contributing to the ED [11]. Since the outer shell with a larger diameter has more atoms for a given length, its diffraction intensity is stronger than that of the inner shell [27].

Thirdly, the (n, m) indices of each shell can be obtained from the layer-line spacing d_k ($k = 1, 2, 3$) from layer-line l_k to l_0 parallel to the tube axis. Geometrically similar to that of SWNTs [22], d_k are directly related to (n, m) indices and diameter D by

$$d_1 = \frac{n-m}{\sqrt{3}\pi}\frac{1}{D}, \qquad d_2 = \frac{n+2m}{\sqrt{3}\pi}\frac{1}{D},$$
$$d_3 = \frac{2n+m}{\sqrt{3}\pi}\frac{1}{D}. \tag{2}$$

Here we note that $d_3 = d_2 + d_1$, which is conveniently used to divide the layer lines into two groups. As l_2 and l_3 correspond to the layer lines with relatively strong intensities and are also far away from layer-line l_0, we choose d_2 and d_3 instead of d_1 for determining the (n, m) from equation (2) to reduce the error. Combining with equation (1), the $(n_o, m_o)/(n_i, m_i)$ of the DWNTs can be calculated by

$$n_o = \frac{\pi}{\sqrt{3}}(2d_{o3} - d_{o2})\left(\frac{1}{e} + \frac{1}{E}\right),$$
$$m_o = \frac{\pi}{\sqrt{3}}(2d_{o2} - d_{o3})\left(\frac{1}{e} + \frac{1}{E}\right), \tag{3a}$$

$$n_i = \frac{\pi}{\sqrt{3}}(2d_{i3} - d_{i2})\left(\frac{1}{e} - \frac{1}{E}\right),$$
$$m_i = \frac{\pi}{\sqrt{3}}(2d_{i2} - d_{i3})\left(\frac{1}{e} - \frac{1}{E}\right). \tag{3b}$$

In principle, equations (3*a*) and (3*b*) are valid only in normal incidence. Under more general conditions, when the tilt angle τ of the nanotube with respect to the electron beam is non-zero (figure 1(*b*)), tilt-effect errors ε_n (defined as $\varepsilon_n = n^{\text{calc}} - n$) will arise. As the intensity distribution of layer-line l_0 is independent of tube tilt [14], the measurement of e and E will not be influenced by tilt angle [27]. The main influence of tilt angle τ on the results comes from the fact that the layer-line spacing d_k is subject to scaling by a factor of $1/\cos\tau$ [15, 22],

Table 1. The tilt-effect error ε_n corresponding to index n under different tilt angle τ. All the conditions that make $\varepsilon_n < 1$ are framed by the bold lines.

	τ				
n	5°	10°	12.5°	15°	20°
5	0.02	0.08	0.12	0.18	0.32
10	0.04	0.15	0.24	0.35	0.64
15	0.06	0.23	0.36	0.53	0.96
20	0.08	0.31	0.49	0.71	1.28
25	0.09	0.39	0.61	0.88	1.60
30	0.11	0.46	0.73	1.06	1.92
40	0.15	0.62	0.97	1.41	2.57
50	0.19	0.77	1.21	1.76	3.21
60	0.23	0.93	1.46	2.12	3.85
70	0.27	1.08	1.70	2.47	4.49
90	0.33	1.38	2.19	3.18	5.76

and so are the calculated (n, m). The tilt-effect errors ε_n can be given by

$$\varepsilon_n = n \cdot (1/\cos\tau - 1) = n^{\text{calc}} \cdot (1 - \cos\tau). \quad (4)$$

Table 1 lists the tilt-effect errors ε_n under different tilt angle τ. It is seen that in most cases ε_n is less than 1, as framed by the bold lines. In particular, when the index n is small ($n \leqslant 15$), ε_n are less than 1 even under a high tilt angle of as large as 20°. Under this condition, ε_n will be very easy to fix. However, error ε_n will increase with increasing index n, and might become considerably large, and even exceed 1. Then the accurate ε_n fixing and (n, m) identification will become tough. This is the general difficulty in the (n, m) assignment of large-indexed nanotubes [18, 26].

Now, let us see how to specify all the tilt-effect errors and evaluate the tilt angle at the same time. From equation (4), the four errors ε_n for a given DWNT under a certain tilt angle τ are directly related to the four calculated indices by

$$\varepsilon_{n_o} : \varepsilon_{m_o} : \varepsilon_{n_i} : \varepsilon_{m_i} = n_o^{\text{calc}} : m_o^{\text{calc}} : n_i^{\text{calc}} : m_i^{\text{calc}}. \quad (5)$$

The tilt-effect error ε_n for the smallest index is first fixed, which is basically less than 1. Then all the other three errors can be specified among the possible values by equation (5). Furthermore, in the case that the errors are determined, the tilt angle τ can be simultaneously evaluated from

$$\cos\tau = 1 - \frac{\varepsilon_{n_o} + \varepsilon_{m_o} + \varepsilon_{n_i} + \varepsilon_{m_i}}{n_o^{\text{calc}} + m_o^{\text{calc}} + n_i^{\text{calc}} + m_i^{\text{calc}}}. \quad (6)$$

With the estimated value of τ, the corresponding simulation of EDPs can be easily carried out to check the assignment results. By using this strategy we can now avoid the complicated trial-and-error procedure with different tilt angles.

In this method, only d_k, e and E measured directly from the EDPs in pixel unit are needed for the (n, m) assignment. Neither any TEM operation parameters, such as the camera length and accelerated voltage, nor C–C bond length are required. Hence, our method is totally calibration-free. In addition, all the information required for the assignment process can be obtained from the peak positions of layer-line l_0 and the first peak positions of layer-line l_2 and l_3. The signal-to-noise ratio (S/N) of these features is the highest in an EDP, which makes (n, m) identification much easier based on the common diffraction patterns. It is also worth noting that this method is applicable for (n, m) determination of commensurate DWNTs of the same chiral angles, with $d_{o3} = d_{i3}$, $d_{o2} = d_{i2}$ and $d_{o1} = d_{i1}$.

3. Results

As the tilt-effect error increases with the increasing index n and tilt angle τ, in order to test the validity of the method, we have simulated the EDP of a large-indexed DWNT under a high tilt angle, i.e. a (60, 50)/(80, 10) DWNT under a tilt angle of as large as 20°, as shown in figure 2(*a*). To measure the layer-line spacing d_k, the integrated layer-line intensities are projected onto the tube axis and plotted as a function of the distance along the tube axis in pixel unit (figure 2(*b*)). The layer lines can be easily divided into groups A and B, according to $d_3 = d_2 + d_1$. It is noted that the intensities of layer-line l_{B1}, l_{B2} and l_{B3} are obviously stronger than layer-line l_{A1}, l_{A2} and l_{A3}, respectively. Group B, therefore, corresponds to the outer tube shell. The two periods of e and E can be directly extracted from the peak positions in layer-line l_0 as illustrated in figure 2(*c*). The measured values and results are all summarized in table 2.

Using equations (3*a*) and (3*b*), the $(n_o, m_o)/(n_i, m_i)$ can be calculated as (64.19, 53.74)/(85.52, 10.67). It deserves to be noted that if we ignore the tilt-effect errors, as adopted in the small-indexed nanotubes, the chiral indices will be determined as (64, 53)/(85, 10), which deviates far from the real indices. In the following, we will show the process of specifying the tilt-effect errors $(\varepsilon_{n_o}, \varepsilon_{m_o}, \varepsilon_{n_i}, \varepsilon_{m_i})$ by considering their relation with the four calculated indices. The error ε_{m_i} of the smallest index 10.67 is first fixed; as discussed above, its value is basically always less than 1. For example, among all the possible values of ε_{m_i} (0.67, 1.67, 2.67, ...), only 0.67 is rational for a real EDP, since the others correspond to a tilt angle of more than 30° (experimentally, $\tau \leqslant 20°$). The error ε_{m_i}can also be conveniently obtained from table 1, as seen in the bold frame area with a value of less than 1. In the case that ε_{m_i} is fixed as 0.67, applying the relation of $\varepsilon_{m_o}/\varepsilon_{m_i} = 53.74/10.67$, ε_{m_o} for the calculated index 53.74 is obtained to be 3.74 among its possible values (..., 2.74, 3.74, 4.74, ...). Similarly, the other two tilt-effect errors for the calculated indices 64.19 and 85.52 can be fitted as 4.19 and 5.52, respectively. Therefore, the tilt-effect errors are fitted as (4.19, 3.74, 5.52, 0.67), and the chiral indices are finally determined as (60, 50)/(80, 10). Simultaneously, the tilt angle can be estimated as 20.9°, according to equation (6), which is in good agreement with the real value of 20°. It shows clearly that the (n, m) of the DWNT can be accurately identified even when the nanotube has an index up to 80 under a high tilt angle of 20°.

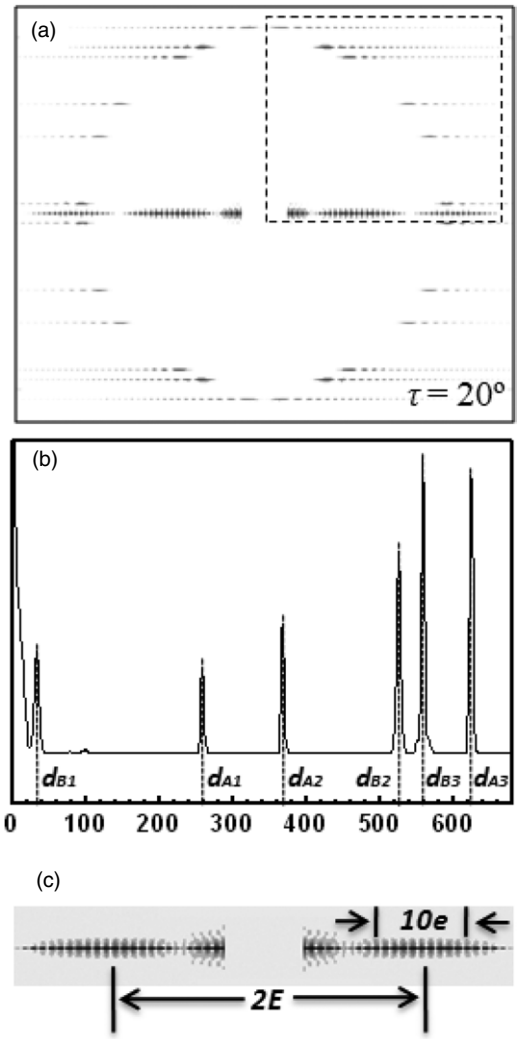

Figure 2. (*a*) Simulated EDP from a (60, 50)/(80, 10) DWNT under a tilt angle of 20°. (*b*) The integrated layer-line intensity projected onto the tube axis corresponding to the framed area in (*a*). Two groups of layer-line spacing d_k can be measured. (*c*) The enlargement of layer-line l_0 and the two oscillation periods of e and E.

Here, we emphasize that only the integrated intensity of layer-line l_2 and l_3 is employed to deduce the (n, m), the details of the intensity distribution are unnecessary in the present method. This is a significant improvement over the several-peak-fitting method [18–20], and makes it easier to index the EDPs.

To apply the method on the (n, m) assignment of real EDPs, isolated ultralong DWNTs were grown across the slit in the SiO_2/Si substrate by ethanol CVD growth, following a procedure similar to the previously reported ultralong SWNTs [28]. The slit substrate was loaded into a JOEL 2010F transmission electron microscope (TEM) operated at 120 kV, through a specialized, home-made specimen holder. Figure 3(*a*) shows a scanning electron microscope (SEM) image of an ultralong DWNT grown on the SiO_2/Si substrate. The nanotube is suspended across the slit. The high-resolution TEM (HRTEM) image of the DWNT obtained at the slit edge is shown in the inset of figure 3(*a*), and the corresponding EDP are presented in the left half of figure 3(*b*). The d_k measured from figure 3(*c*), e and E extracted from figure 3(*d*) and the determined chiral indices are summarized in table 3.

The same procedure used above for the (n, m) assignment in the simulated EDPs is adopted. Layer-line group A is recognized to correspond to the outer tube shell, since the integrated intensity of layer-line group A is stronger than that of group B. The $(n_o, m_o)/(n_i, m_i)$ indices are calculated as (48.80, 6.08)/(34.56, 13.15). Similarly, the tilt-effect error ε_{m_o} for the smallest index 6.08 is first fixed as 0.08, and then other three errors ε_{n_o}, ε_{n_i} and ε_{m_i} can be fixed as 0.80, 0.56 and 0.15, respectively. Finally the chiral indices are determined as (48, 6)/(34, 13), and the tilt angle can be estimated as 10.1°. We have simulated the EDP (figure 3(*b*) right) based on the identified (n, m) around the estimated tilt angle, using the Matlab code similar to the analysis of graphite cones and muti-walled CNTs in our group [29, 30]. We found that the best fitting EDP is under a tilt angle of 9.6°, which is very close to the estimated value.

Besides extracting e and E from the peak positions in layer-line l_0, we can also fit its intensity profile by a mathematical expression [25],

$$I_0(R) \propto |J_0(\pi D_o R) + J_0(\pi D_i R)|^2. \tag{7}$$

Figure 4 shows the intensity fitting of layer-line l_0 for the EDP in figure 3(*b*), with the best fitting e and E values to 31.85 and 319.0, respectively. These values are very close to what we directly extracted from the peak positions.

4. Discussion

First, the possible error for this method should be considered. As the absolute value of e is much smaller than d_k and E, the major source of errors should come from the measurement error of e, especially the relative small magnitude of e as a divisor in equations (3*a*) and (3*b*). Since e is inversely proportional to the average diameter ($\bar{D}$) of the DWNTs, as for the small-indexed nanotubes with small $\bar{D}$, the value of e is relatively large and the corresponding measurement error is negligible. As for the large-indexed nanotubes, the measurement error of e becomes notable. In such cases, $1/e$ is much larger than $1/E$ ($1/e \propto \bar{D}$, $1/E \propto \delta$D, $\bar{D} \geqslant \delta$D), and the four calculated indices from equations (3*a*) and (3*b*) and four tilt-effect errors from equation (4) are all approximately in proportion to e. In the error-fixing procedure, the proportional relationship between the four errors is adopted to identify the tilt-effect errors. Therefore the measurement error of e only makes the tilt-effect errors deviate from the real value, but the final identified chiral indices are accurate. We find out that the largest tolerated e error is 2% for small-indexed nanotubes but 5–10% for large-indexed nanotubes ($n > 30$). This is a significant progress in comparison with the previous method, in which all the values have to be measured with critically high precision.

Secondly, the proposed method is widely valid. This method is based on accurately fixing the tilt-effect errors by considering their relationship with the correspondingly calculated chiral indices. In the case that the smallest error $\varepsilon_{\min}$

Table 2. Measured d_k, e, E and calculated results of the simulated EDP in figure 2(*a*).

	d_1	d_2	d_3	E	e	$(n_o,m_o)/(n_i, m_i)$	$(\varepsilon_{n_o}, \varepsilon_{m_o}, \varepsilon_{n_i}, \varepsilon_{m_i})$	τ_{calc}
Group A	257	367	624	309.5	17.62	(64.19, 53.74)/	(4.19, 3.74,	20.9°
Group B	32	526	558			(85.52, 10.67)	5.52, 0.67)	

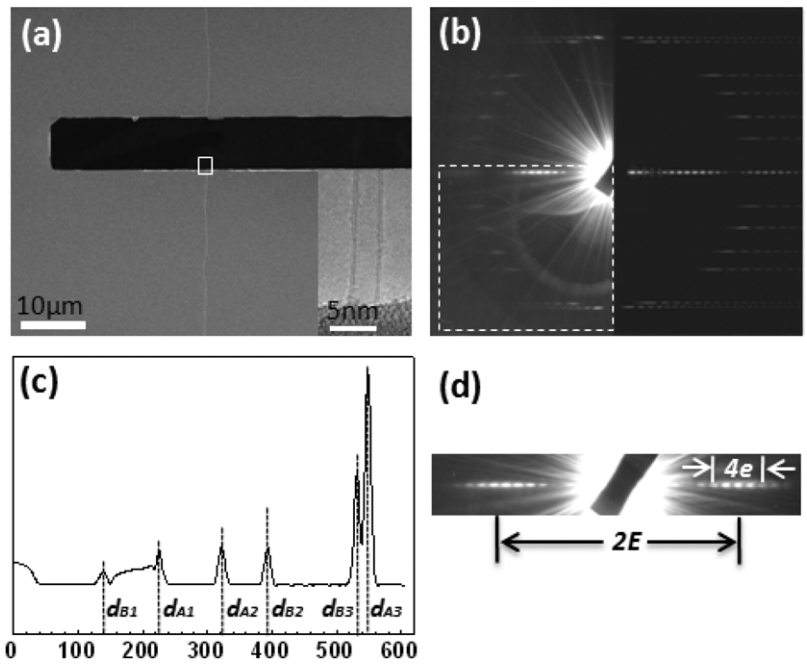

Figure 3. (*a*) SEM image of an isolated ultralong DWNT grown onto the SiO_2/Si slit substrate. The inset is the HRTEM image of the nanotube, acquired in the region as marked by the frame at the slit edge. (*b*) The corresponding experimental (left) and simulated (right) EDP of the same DWNT. (*c*) The integrated layer-line intensity corresponding to the framed area in (*b*). The background has been subtracted. (*d*) The enlargement of layer-line l_0 and the two oscillation periods of e and E.

Table 3. Measured d_k, e, E and calculated results from the experimental EDP in figure 3(*b*).

	d_1	d_2	d_3	E	e	$(n_o, m_o)/(n_i, m_i)$	$(\varepsilon_{n_o}, \varepsilon_{m_o}, \varepsilon_{n_i}, \varepsilon_{m_i})$	τ_{calc}
Group A	227	324	551	319.0	31.80	(48.80, 6.08)/	(0.80, 0.08,	10.1°
Group B	139	395	534			(34.56, 13.15)	0.56, 0.15)	

for the calculated index is fixed, the others can be subsequently fixed with high resolution. In most cases, it is very convenient to fix ε_{min}, since its value is usually less than 1. As a matter of fact, the largest index n that keeps $\varepsilon_{min} < 1$ is around 60 if tilt angle τ is less than 10°. In actual practice, we can tilt the specimen holder to ensure $\tau \leqslant 10°$. In the literature, the experimental tilt angle is usually in the range $0° \leqslant \tau \leqslant 20°$ [18, 21], and occasionally reaches 30°. Without loss of the generality of this method, we suppose the $0° \leqslant \tau \leqslant 40°$. If we record several EDPs under angles −30°, 0° and 30° of the specimen holder with respect to the nanotube axis, one of them is taken under $\tau \leqslant 10°$. This practice is very similar to taking a series of HRTEM images to obtain the best focus conditions. Thus it is very easy for our method to identify the CNTs with the smallest index less than 60, which covers almost all of the nanotubes that we are interested in the study on individual nanotubes. In the utmost limit, if the smallest index error is not less than 1 even after tilting the specimen holder, the trial-and-error procedure will be applied. Since the tilt angle is highly sensitive to the determined tilt-effect errors, the wrong tilt-effect error will lead the estimated tilt angle to deviate far from the real value. Thus the simulated EDPs under the tilt angle will appear inconsistent with the experimental ones. Then we add 1 to ε_{min} and retrieve the chiral indices again.

Finally, the method developed here can also be expanded to the (n, m) assignment of SWNTs and other few-walled nanotubes. As for SWNTs, this is only a period e in the intensity distribution of layer-line l_0. We can consider that the E is infinite or $1/E$ is zero in equations (3*a*) and (3*b*), and this is just the case reported in [22]. As for other few-walled nanotubes, for example a three-walled nanotube, the three diameters for different shells can be identified by fixing the intensity profile of layer-line l_0, and the following procedure is similar to that before. Additionally, as this method is calibration-free for the atom bonding length, it can also be applied to other kinds of cylindrical nanotubes, such as boron-nitride nanotubes [31].

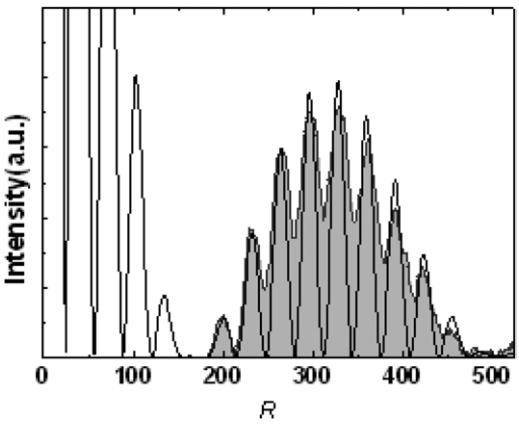

Figure 4. Bessel function fitting to the intensity profile of layer-line l_0 of the EDP in figure 3(*b*) with parameters of $e = 31.85$ and $E = 319.0$.

5. Conclusion

To sum up, we have developed an efficient method to directly determine the chiral indices of DWNTs by EDPs. With careful consideration of the relationship between the tilt-effect errors and the corresponding calculated chiral indices, the unique procedure in determining the atomic structure of the large-indexed nanotubes under a high tilt angle has been fully demonstrated in the simulated and experimental EDPs. Since this method only employs the peak positions in layer-line l_0 and the integrated intensity in layer-line l_2 and l_3, the chiral index determination of common diffraction patterns is accessible. Our method can also be applied to other types of CNTs, such as SWNTs and few-walled nanotubes, and other kinds of cylindrical nanotubes, such as boron-nitride nanotubes.

Acknowledgments

The authors thank Professor L-C Qin for the grateful discussion at the initial stage of this work. K H Liu is grateful to Mr Yagang Yao for preparing the DWNT samples. This work is supported by the NSF (Nos 50725209 and 60621091), MOST (Nos 2007CB936203 and 2007AA03Z353) and CAS of China.

References

[1] Iijima S 1991 *Nature* **354** 56
[2] Baughman R H, Zakhidov A A and de Heer W A 2002 *Science* **297** 787
[3] Hamada N, Sawada S and Oshiyama A 1992 *Phys. Rev. Lett.* **68** 1579
[4] Saito R, Dresselhaus G and Dresselhaus M S 1998 *Physical Properties of Carbon Nanotubes* (London: Imperial College Press)
[5] Wildoer J W G, Venema L C, Rinzler A G, Smalley R E and Dekker C 1998 *Nature* **391** 59
[6] Jorio, Saito R, Hafner J H, Lieber C M, Hunter M, McClure T, Dresselhaus G and Dresselhaus M S 2001 *Phys. Rev. Lett.* **86** 1118
[7] Hashimoto A, Suenaga K, Urita K, Shimada T, Sugai T, Bandow S, Shinohara H and Iijima S 2005 *Phys. Rev. Lett.* **94** 045504
[8] Iijima S and Ichihashi T 1993 *Nature* **363** 603
[9] Cowley J M, Nikolaev P, Thess A and Smalley R E 1997 *Chem. Phys. Lett.* **265** 379
[10] Qin L-C, Ichihashi T and Iijima S 1997 *Ultramicroscopy* **67** 181
[11] Lambin P and Lucas A A 1997 *Phys. Rev.* B **56** 3571
[12] Amelinckx S, Lucas A and Lambin P 1999 *Rep. Prog. Phys.* **62** 1471
[13] Qin L-C 2006 *Rep. Prog. Phys.* **69** 2761
[14] Qin L-C 2007 *Phys. Chem. Chem. Phys.* **9** 31
[15] Gao M, Zuo J M, Twesten R D, Petrov I, Nagahara L A and Zhang R 2003 *Appl. Phys. Lett.* **82** 2703
[16] Liu Z J, Zhang Q and Qin L-C 2005 *Phys. Rev.* B **71** 245413
[17] Meyer J C, Paillet M, Duesberg G S and Roth S 2006 *Ultramicroscopy* **106** 176
[18] Jiang H, Brown D P, Nasibulin A G and Kauppinen E I 2006 *Phys. Rev.* B **74** 035427
[19] Liu Z J and Qin L-C 2005 *Chem. Phys. Lett.* **408** 75
[20] Zuo J M, Kim T, Celik-Aktas A and Tao J Z 2007 *Angew. Math. Mech.* **222** 625
[21] Colomer J F, Henrard L, Launois P, Van Tendeloo G, Lucas A A and Lambin P 2004 *Phys. Rev.* B **70** 075408
[22] Jiang H, Nasibulin A G, Brown D P and Kauppinen E I 2006 *Carbon* **45** 662
[23] Zuo J M, Vartanyants I, Gao M, Zhang R and Nagahara L A 2003 *Science* **300** 1419
[24] Gao M, Zuo J M, Zhang R and Nagahara L A 2006 *J. Mater. Sci.* **41** 4382
[25] Kociak M, Suenaga K, Hirahara K, Saito Y, Nakahira T and Iijima S 2002 *Phys. Rev. Lett.* **89** 155501
[26] Kociak M, Hirahara K, Suenaga K and Iijima S 2003 *Eur. Phys. J.* B **32** 457
[27] Hirahara K, Kociak M, Bandow S, Nakahira T, Itoh K, Saito Y and Iijima S 2006 *Phys. Rev.* B **73** 195420
[28] Yao Y G, Li Q W, Zhang J, Liu R, Jiao L Y, Zhu Y T and Liu Z F 2007 *Nature Mater.* **6** 283
[29] Zhang G Y, Jiang X and Wang E G 2003 *Science* **300** 472
[30] Xu Z, Bai X, Wang Z L and Wang E G 2006 *J. Am. Chem. Soc.* **128** 1052
[31] Golberg D, Bando Y, Bourgeois L, Kurashima K and Sato T 2000 *Appl. Phys. Lett.* **77** 1979